Polymer Journal (2019) 51:795–801
https://doi.org/10.1038/s41428-019-0194-3

NOTE

Energy storage behaviors in ferroelectric capacitors fabricated with sub-50 nm poly(vinylidene fluoride) Langmuir–Blodgett nanofilms

Huie Zhu[1] · Tokuji Miyashita[1] · Masaya Mitsuishi[1]

Received: 23 November 2018 / Revised: 25 March 2019 / Accepted: 26 March 2019 / Published online: 23 April 2019

Abstract

High-energy storage in polymer dielectrics is limited by two decisive factors: low-electric breakdown strength and high hysteresis under high fields. Poly(vinylidene fluoride) (PVDF), as a well-known ferroelectric polymer having a high-breakdown strength (700 MV/m) and a high dielectric constant, is suitable for use as a dielectric capacitor film, but ferroelectric hysteresis from the crystalline phase has prevented its practical application. In our previous study, the ferroelectric switching of crystalline PVDF is suppressed effectively in PVDF-based Langmuir–Blodgett (LB) nanofilms because of its large interfacial effect, even in an extremely high electric field. This study investigated the ferroelectricity and energy storage behaviors of PVDF LB nanofilms at sub-50 nm thicknesses. The ferroelectric hysteresis loops were measured using a Sawyer–Tower circuit in different electric fields. An energy density of 6.0 J/cm^3 at 500 MV/m was demonstrated for the 12-nm-thick PVDF LB nanofilm device.

Introduction

Polymer dielectrics have attracted much attention because of their low weight, high-breakdown strength, and great reliability and scalability [1]. High-energy density and low-loss dielectrics are urgently demanded and require a (1) high permittivity, (2) high-electronic breakdown strength (field), (3) low-dissipation factor under low fields, and (4) low hysteresis between 10 Hz and a few hundred kHz [2]. Polymer dielectrics are therefore promising for next generation energy-storage applications such as wind power and hybrid and electric vehicles [3]. Polar polymers with permanent dipoles are suitable for use as high-energy storage density dielectrics because of their high permittivity. One such polymer is poly(vinylidene fluoride) (PVDF), with its distinctively large dielectric constant (k~ 10) that is superior to those of other dielectric polymers. Unfortunately, the large dielectric loss in high-k PVDF (tan δ~ 0.02) hampers its application. That loss is 1000 times greater than that of the typical commercial polymer dielectric films (k~ 3, tan δ~ 0.0002) made from biaxially oriented polypropylene [4]. Suppressing the dielectric hysteresis loss and increasing the energy storage density and charge–discharge efficiency require the manipulation of the PVDF crystallization, including preferential crystallization and miniaturization of the crystal size [5, 6].

As a semicrystalline polymer, several crystalline forms exist in PVDF materials, including the most common form-I (β) and form-II (α). Reportedly, each crystal form has a different potential energy; those of the β and α phases are, respectively, −5.73 and −6.03 kcal/monomer unit [7]. Therefore, PVDF usually crystallizes into the thermodynamically stable α phase in which the molecular chains take a trans-gauche–trans-gauche (TGTG) conformation and generate a zero net dipole. Thereby, no corresponding electric polarization is generated [8]. By contrast, under extreme conditions such as high electric field poling, ferroelectric β-crystal domains with an all-trans molecular conformation will be produced, with a bistable intrinsic polarization that can be switched by the application of a reversal electric field. For energy storage applications, coupling interactions among

Supplementary information The online version of this article (https://doi.org/10.1038/s41428-019-0194-3) contains supplementary material, which is available to authorized users.

✉ Huie Zhu
zhuhuie@tohoku.ac.jp

✉ Masaya Mitsuishi
masaya@tohoku.ac.jp

[1] Institute of Multidisciplinary Research for Advanced Materials, Tohoku University, 2-1-1 Katahira, Aoba-ku, Sendai 980-8577, Japan

the PVDF β domains and competition between the polarization and depolarization fields affect the dipole reorientation and energy storage properties. PVDF materials with a high content of β phase and small β-domain size with discontinuous domain boundaries are useful for higher energy storage and low loss because the domain coupling interactions are weakened to ease the switching back of the aligned dipole in the β domains once the external electric field is removed. To realize that weak coupling interaction, the reduction of the PVDF film thickness below 100 nm is one effective method, but it is extremely difficult because almost all traditional top-down methods such as mechanical stretching will lose their function at the sub-100-nm thickness scale [9].

In our earlier work, we proposed a facile bottom-up method to prepare a PVDF quasi-monolayer (~2.3 nm) at the air–water interface, which can be transferred repeatedly with nanometer-scale precision onto various substrates for multilayered PVDF Langmuir–Blodgett (LB) nanofilms [10]. FT-IR measurements demonstrated that the β-crystal content in the PVDF LB nanofilms reached 95%, one of the highest values ever reported. The total crystallinity was moderate, as high as 50%, which is comparable to that of bulk PVDF. The PVDF nanofilms provide extraordinary ferroelectricity when used as an insulating layer in electronic devices such as resistive switching nonvolatile memories and spin valves [6, 11, 12]. These unique PVDF LB nanofilm properties make them possible as high-electric density and low-loss dielectrics because of their well-defined nanoscale layer structures. Because of the precisely controllable film thickness and the predominance of electroactive β crystals in PVDF LB nanofilms, one can clarify the ferroelectric behaviors and energy storage properties of sub-50 nm ultrathin films, which is very challenging when using traditional methods. A nonlinear dielectric with a high dielectric constant, high-electric breakdown strength, and low hysteresis under high fields are required to achieve a high-energy storage density. For this study, we used the Sawyer–Tower method to demonstrate the ferroelectricity and energy storage properties of ferroelectric capacitors with a sandwich device structure of Al/sub-50-nm-thick PVDF nanofilm/Al.

Experimental section

Materials

PVDF ($M_n = 7.1 \times 10^4$, $M_w/M_n = 2.5$; Aldrich Chemical Co. Inc.) was reprecipitated once before use. Amphiphilic poly(*N*-dodecylacrylamide) (pDDA) ($M_n = 3.0 \times 10^4$, $M_w/M_n = 3.0$) was used as a stabilizer of the PVDF monolayer formation at the water surface. The pDDA was synthesized through free radical polymerization from *N*-dodecylacrylamide initiated by AIBN, referring to a method described in an earlier report [13]. Solvents including *N*-methyl-2-pyrrolidone (NMP) and chloroform were commercially available. They were used without further purification for the LB film preparation. Octyltrichlorosilane was purchased from Tokyo Chemical Industry Co. Ltd. for the hydrophobic treatment of the substrate surfaces. Slide glasses were purchased from Matsunami Glass Ind. Ltd., Japan. Aluminum wire was obtained from the Nilaco Corp., Japan.

Preparation of PVDF LB nanofilms

The LB film preparation was described in our previous work [10, 14]. Briefly, PVDF and pDDA were dissolved respectively in NMP and chloroform at room temperature with solution concentrations of ca. 1 mM. The two resultant solutions of pDDA and PVDF were then spread successively onto the water surface to form a stable mixed Langmuir film at a molar mixing ratio of PVDF:pDDA = 50:1 (Fig. 1a). The surface pressure (π)–area (A) isotherm was recorded automatically during the compression of the molecules by a PTFE bar. The surface pressure was kept at 30 mN/m for monolayer transfer (Fig. 1b). During the deposition, the substrate holder was lifted at a dipping speed of 10 mm/min in both upstrokes and downstrokes. The dominant formation of the ferroelectric β crystal (>95%) (an orthorhombic unit cell with lattice constants of $a = 8.45$ Å, $b = 4.88$ Å, and $c = 2.55$ Å) was also demonstrated.

Device fabrication

The ferroelectric capacitors were fabricated with a sandwich structure of aluminum (Al)/ PVDF LB nanofilm/aluminum (Al) by the following steps (Fig. 2a). *Step* 1: Bottom Al bar electrodes as thick as 40 ± 5 nm with a width of 3 mm were thermally evaporated through a metal mask at a rate of 1.0 Å/s onto clean glass substrates (TSU062H; Balzers, Germany). *Step* 2: The PVDF monolayers were transferred repeatedly from the air–water interface onto the Al-coated glass substrates with three layer numbers of 5, 15, and 25, designated as 5LB, 15LB, and 25LB. *Step* 3: The top electrode was then deposited using a similar method to that of *Step* 1, but the metal mask was aligned in an orthogonal orientation. The LB films were protected from burning by liquid nitrogen cooling during the top electrode Al evaporation.

Results and discussion

Surface morphologies of PVDF LB nanofilms on an Al electrode

The device fabrication process, which is presented schematically in Fig. 2a, is described in the experimental

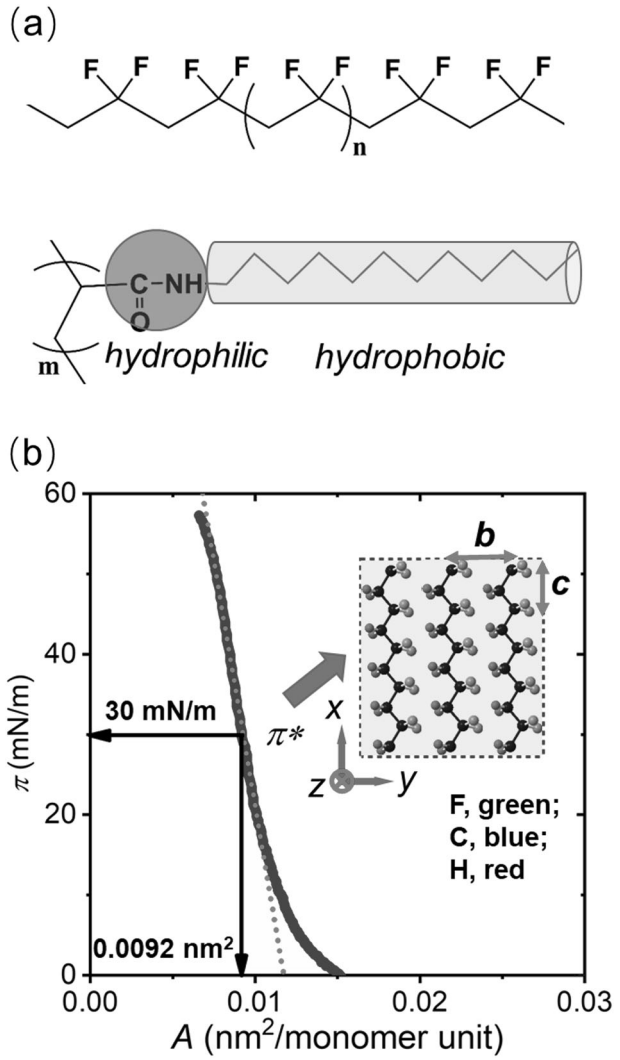

Fig. 1 **a** Chemical structures of PVDF and pDDA and **b** surface pressure (π)–area (A) isotherm of PVDF monolayer, where π^* denotes the condensed monolayer state. The inset presents a schematic view of the PVDF molecular packing in the monolayer at the water surface. The cross mark denotes the direction vertical to the water surface. The x–y plane is the water surface. The letters b and c are the crystal lattices of the PVDF β crystals (b//monomer dipole)

section. Aluminum was selected for the top and bottom electrodes because it easily forms a surface oxidation dead layer, causing a depolarization field in ferroelectric films and hindering a fast polarization reversal and current leakage [15]. We prepared a series of devices with a sandwiched capacitor structure of Al/PVDF LB nanofilm/Al by varying the number of deposited layers to 5, 15, and 25. The surface morphologies of the Al bottom electrode and PVDF LB nanofilms with different numbers of layers are shown in Fig. 2b–e. The bottom Al electrode showed a smooth surface with a root mean square surface roughness of 3.7 nm (Fig. 2b). After the PVDF nanosheet deposition, the surface morphologies became rougher, indicating the successful deposition of the PVDF monolayer from the air–water interface. As shown in AFM images, PVDF nanofibers were formed with the average diameters of 21, 21, and 24 nm, respectively, for 5LB, 15LB, and 25 LB (Fig. 2c–e). The results further prove that our method controlled the film deposition precisely and that the crystal domain was confined in the nanofibers with smaller size. It is apparent that the fiber number increased as the deposition cycles increased, which contributed to the overlaying of the nanofibers. Because the average monolayer thickness was determined as 2.3 nm using a cross-sectional AFM image, as presented in Fig. 2f, the corresponding thicknesses for the different films of 5LB, 15LB, and 25LB were, respectively, 12, 35, and 58 nm [10].

Ferroelectric hysteresis loop measurements

We used a homemade Sawyer–Tower circuit to evaluate the as-prepared ferroelectric capacitors, with no post treatment, and assess their ferroelectricity (Fig. 3). The circuit has two capacitors in series, including the reference capacitor (C_r) and the ferroelectric capacitor (C_f), which share the charge that passes between them (Q). The voltage through the reference capacitor (V_r) can be recorded using an oscilloscope. Therefore, the Q value is equal to C_rV_r, which is useful for calculating the electric polarization value at the ferroelectric capacitor if the electrode area (A) is known (Eqn. 1). In this study, a triangle waveform voltage with a frequency of 10 Hz was applied to the reference capacitor with a capacitance value of 1 μF. The voltage magnitude was changed gradually for the different samples.

$$D = \frac{C_rV_r}{A} \tag{1}$$

Dielectric materials are electric insulators through which no electric charge can pass freely. Instead, dielectric polarization is induced by an applied electric field, resulting in the accumulation of positive charges on one side and negative charges on the opposite side. These accumulated charges enable electric charge storage [16]. The polymer dielectrics include linear and nonlinear types, which respectively demonstrate linear and nonlinear electric displacement (D) responses to an applied effective electric field (E), obtained by considering the induced voltage across the reference capacitor from the applied electric field. Considering the easy oxidation of the aluminum electrodes, especially the bottom electrode, the depolarization electric field is another important factor that influences the final hysteresis loops. Figure 4a–c shows the final electric displacement (D)-electric field (E) hysteresis loops that results after considering the effects of both the induced voltage across the reference capacitor and the depolarization electric field from the interfacial oxide layer [6]. The calculation details

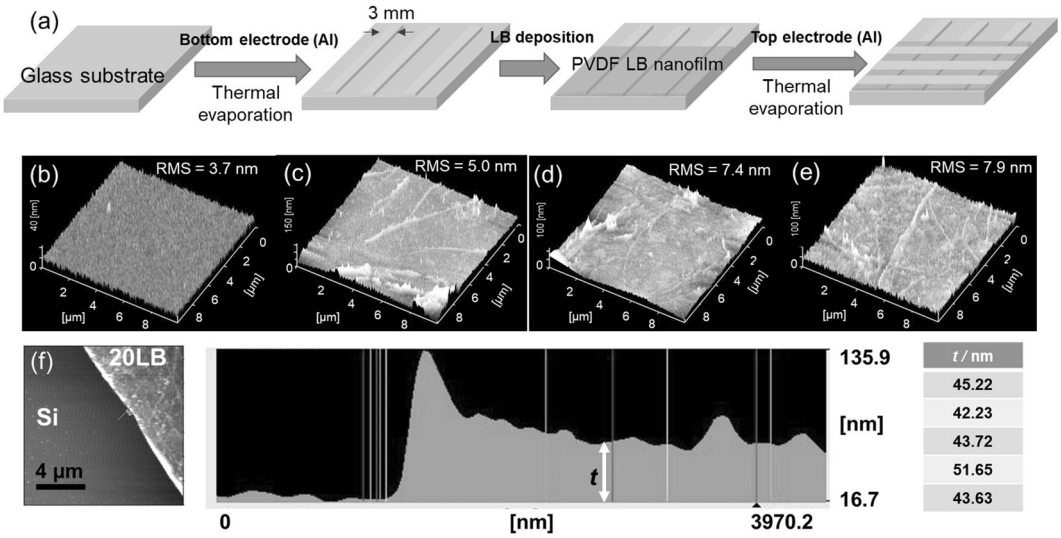

Fig. 2 **a** Schematic illustration of device fabrication process and surface morphologies of the **b** Al bottom electrode, **c** 5-layer PVDF (5LB), **d** 15-layer PVDF (15LB), and **e** 25-layer PVDF (25LB), obtained using atomic force microscopy (scale bar: 2 μm), and **f** the cross-sectional AFM images of a 20-layer PVDF LB nanofilm on a silicon substrate The height information is listed in the bottom-right table for each line in the AFM profile image

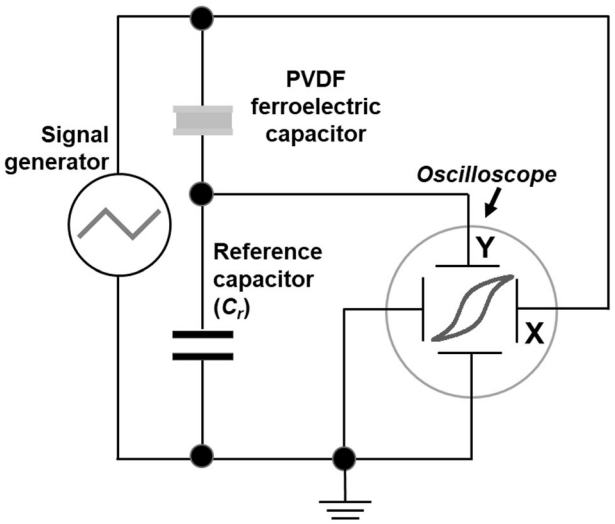

Fig. 3 Schematic illustration of Sawyer–Tower circuit for ferroelectric hysteresis measurement

are depicted in the supplementary information. Under a low electric field, the dielectric behavior was demonstrated to be that of a linear-type dielectric because the electric field was sufficient to polarize mobile amorphous dipoles but was not sufficiently strong to polarize the crystalline dipoles in the PVDF LB nanofilms [16]. Therefore, at the discharge stage, the polarized dipole easily reverted to its original state, following its charge curve. Under stronger electric fields, the dipole orientation in the crystalline domains can be aligned along the electric field. However, the discharge process could not revert all the polarized crystals back to their original states, thereby giving rise to nonlinear *D–E* hysteresis loops and remanent polarizations (a polarization value at a zero electric field, Fig. 4a). However, as the film thickness increased, the hysteresis loop gradually grew to a more saturated shape because the effect of the depolarization field originating from the interfacial Al_2O_3 layer on the ferroelectric polarization became weaker. The remanent (P_r) and spontaneous (P_s) polarization values are presented in Fig. 4d. It is readily apparent that both the P_r and P_s values increase with the electric field magnitude until the electric field reaches its maximum electrical strength. The non-saturated behavior can also be interpreted in terms of the interfacial depolarization field and the limited crystallinity (50%) [10, 17]. The asymmetric hysteresis loops of the 5LB films (4 and 5 V, Fig. 4a) also imply that interfacial effects become more prominent as the film thickness decreases [18].

Energy storage behaviors

To characterize the energy storage properties of dielectrics, *D–E* loops are commonly used. For linear dielectrics, the charge curves always follow the discharge curves, as there is no hysteresis loss. The stored energy density can be released effectively, as shown in Eqn. 2, where ε_r and ε_0 respectively denote the relative dielectric constant and the vacuum permittivity. However, the discharge curve in nonlinear dielectrics (ferroelectrics) does not follow the charge curve because the remanent polarization generates unreleased energy, which is the energy loss (Fig. 5a). The energy stored (U_{nl}) and energy loss (U_{loss}) are marked clearly. In this case, the stored energy density is expressed as Eqn. 3, and the charge–discharge efficiency (η) in nonlinear dielectrics is expressed as Eqn. 4. According to these equations, a

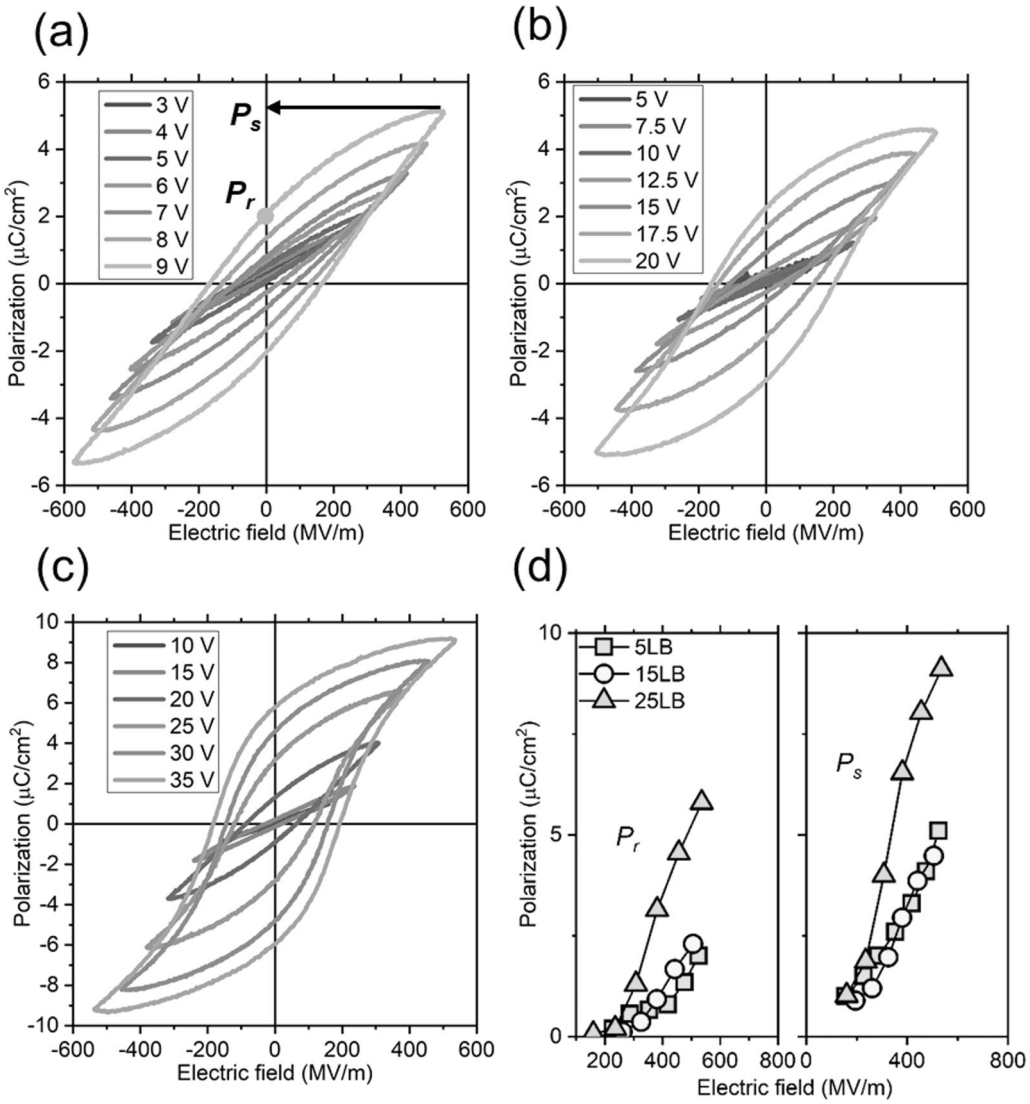

Fig. 4 Ferroelectric hysteresis loops at varying external applied voltages of **a** 5LB, **b** 15LB, **c** 25 LB, and **d** variations of the remanent polarization (P_r) and spontaneous polarization (P_s) with different electric field

nonlinear dielectric with a high dielectric constant, high-electric breakdown strength, and low hysteresis under high fields are required to achieve a high-energy storage density. The dielectric constant and breakdown strength of PVDF are reportedly as high as 10–12 and 700 MV/m, respectively, for bulky materials at room temperature [5].

$$U_l = \int EdD = 0.5\varepsilon\varepsilon_0 E^2 \tag{2}$$

$$U_{nl} = \int EdD \neq 0.5\varepsilon(E)\varepsilon_0 E^2 \tag{3}$$

$$\eta = \frac{U_{nl}}{U_{nl} + U_{loss}} \tag{4}$$

In these equations, E, D, ε, and ε_0, respectively, represent the electric field, electric displacement, dielectric constant, and permittivity.

The details of the energy storage behaviors were investigated for these ferroelectric capacitors. We show the stored energy as a function of the electric field for each sample (Fig. 5b). These results show the distinct possibility of achieving a high-energy storage density in our devices. All the devices exhibited similar trends: the energy density stored increased as the electric field increased. The highest energy stored was 6.0 J/cm^3 (5LB) at 500 MV/m, which is comparable to those of most polymer-based dielectrics [16, 19, 20]. On the other hand, the energy loss invariably increased as the electric field and the film thickness increased because of the increased remanent polarization (Fig. 5c). The small β-crystal size is beneficial for the suppression of hysteresis-induced dielectric loss because the ferroelectric domain coupling can be "nanoconfined" at discontinuous boundaries, in which the polarized domain

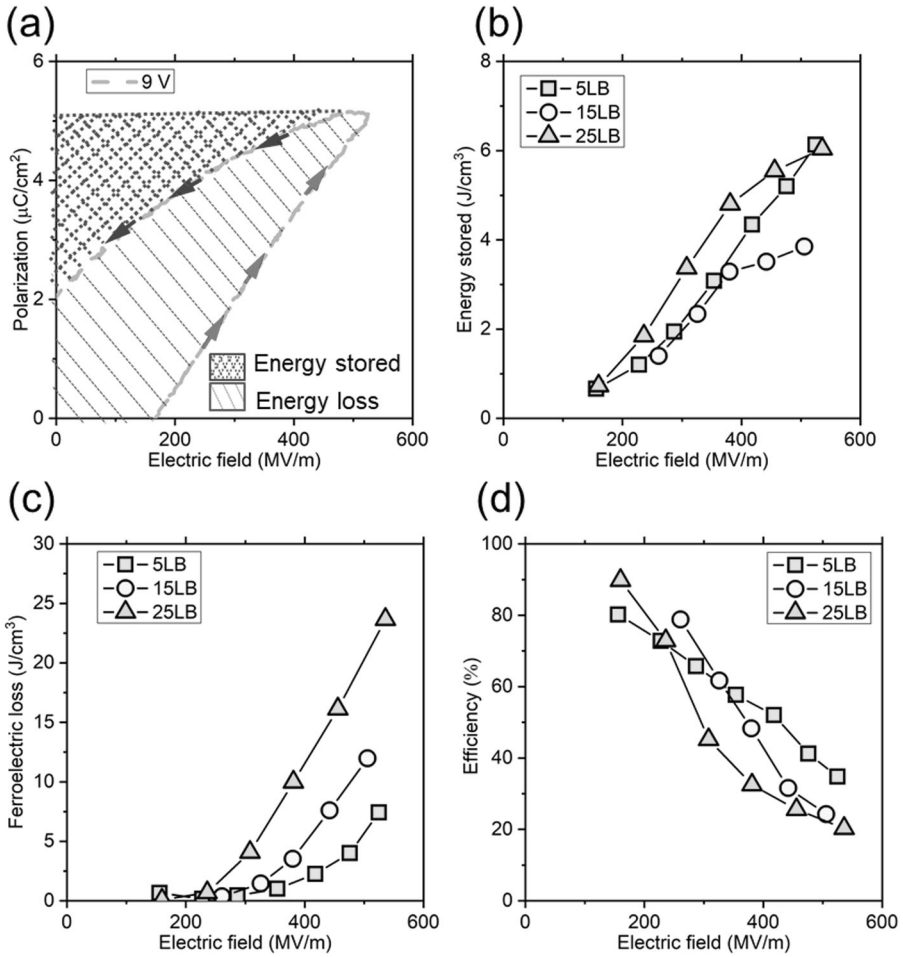

Fig. 5 **a** Schematic description of the energy storage characteristics for the 5LB capacitor induced by a triangle-wave AC voltage with a 9 V amplitude, **b** the calculated energy storage density, **c** the ferroelectric energy loss, and **d** the discharged energy efficiency for each sample

readily switches back to its original state once removed from the external electric field. The fewer PVDF nanofibers in the thinner film (5LB) provide more limited space for the growth of the β-crystal domains under the external electric field than in the thicker films. However, the domain coupling interactions might be hindered by the surrounding pDDA materials, which can explain the easy dipole reorientation. Therefore, the thinner films gave rise to a lower remanent polarization and a lower dielectric loss. The charge–discharge efficiency (η) of the devices is presented in Fig. 5d. It is noteworthy that the 5LB devices proved to have the highest efficiency over the thicker devices because of their slim hysteresis. The efficiency value for 25LB decreases from 90% to 20% as the electric field increases, which might be ascribed to the greater energy loss induced by the ferroelectric hysteresis with higher remanent polarization and the current leakage from the breakdown of the pDDA component, which was observed as the electric breakdown strength of 270 MV/m [21]. These results suggest that the nano-confinement-induced miniaturization of the PVDF crystal size can enhance energy storage behaviors in ferroelectric dielectrics. We also confirmed the D–E curves of pDDA using the same Sawyer–Tower circuit. There was no output response observed. During the film preparation, only a tiny amount of pDDA was used, with a molar ratio of PVDF:pDDA = 50:1. The main function of the pDDA is to stabilize the monolayer formation of PVDF at the air–water interface. Therefore, the pDDA may have little effect on the final energy storage. It is expected to be instructive, in future studies, to develop PVDF monolayers by mixing inorganic nanomaterials and dielectric polymers with a high-electric strength [3].

Conclusions

In summary, PVDF LB nanofilms with thicknesses of less than 60 nm were studied for use in ferroelectric energy storage capacitors. PVDF LB nanofilms have a unique layer structure consisting of amorphous PVDF and nanofiber-structured (crystalline) PVDF components surrounded by amphiphilic pDDA, which is suitable for high-energy density and low-loss dielectric investigations. A series of ferroelectric hysteresis loops were obtained for devices in different electric

fields. The highest energy stored was 6.0 J/cm^3 for a film with a thickness of 12 nm, with a charge–discharge efficiency of 34.8%. This was the first report that depicts the energy storage behavior of ferroelectric devices at such a thickness scale. Though surface effects such as the local depolarization field, surface roughness, and crystallinity should be clarified in detail [18], an even higher energy storage density can be achieved for our devices after device optimization.

Acknowledgments The work was partially supported by Grants-in-Aid for Young Scientists (B) (16K17953) and Scientific Research (B) (16H04197) from the Japan Society for the Promotion of Science (JSPS). The work was also supported by the Cooperative Research Program "Network Joint Research Center for Materials and Devices": Dynamic Alliance for Open Innovation Bridging Human, Environment and Materials (MEXT), the Morinomiyako Project for Empowering Women in Research, the Tohoku University Center for Gender Equality Promotion (TUMUG), and the TAGEN project, Tohoku University. MM thanks the Nohmura Foundation for Membrane Structure's Technology for financial support.

Compliance with ethical standards

Conflict of interest The authors declare that they have no conflict of interest.

References

1. Li Q, Chen L, Gadinski MR, Zhang S, Zhang G, Li HU, et al. Flexible high-temperature dielectric materials from polymer nanocomposites. Nature. 2015;523:576–9.
2. Mackey M, Schuele DE, Zhu L, Flandin L, Wolak MA, Shirk JS, et al. Reduction of dielectric hysteresis in multilayered films via nanoconfinement. Macromolecules. 2012;45:1954–62.
3. Prateek Thakur VK, Gupta RK. Recent progress on ferroelectric polymer-based nanocomposites for high energy density capacitors: synthesis, dielectric properties, and future aspects. Chem Rev. 2016;116:4260–317.
4. Baer E, Zhu L. 50th anniversary perspective: dielectric phenomena in polymers and multilayered dielectric films. Macromolecules. 2017;50:2239–56.
5. Guan F, Wang J, Pan J, Wang Q, Zhu L. Effects of polymorphism and crystallite size on dipole reorientation in poly(vinylidene fluoride) and its random copolymers. Macromolecules. 2010;43:6739–48.
6. Zhu H, Yamamoto S, Matsui J, Miyashita T, Mitsuishi M. Ferroelectricity of poly(vinylidene fluoride) homopolymer Langmuir–Blodgett nanofilms. J Mater Chem C. 2014;2:6727–31.
7. Hasegawa R, Kobayashi M, Tadokoro H. Molecular conformation and packing of poly(vinylidene fluoride). Stability of three crystalline forms and the effect of high pressure. Polym J. 1972;3:591–9.
8. Furukawa T. Ferroelectric properties of vinylidene fluoride copolymers. Phase Transit. 1989;18:143–211.
9. Nasir M, Matsumoto H, Minagawa M, Tanioka A, Danno T, Horibe H. Formation of β-phase crystalline structure of PVDF nanofiber by electrospray deposition: additive effect of ionic fluorinated surfactant. Polym J. 2007;39:670–4.
10. Zhu H, Mitsuishi M, Miyashita T. Facile preparation of highly oriented poly(vinylidene fluoride) Langmuir–Blodgett nanofilms assisted by amphiphilic polymer nanosheets. Macromolecules. 2012;45:9076–84.
11. Zhu H, Yamamoto S, Matsui J, Miyashita T, Mitsuishi M. Resistive non-volatile memories fabricated with poly(vinylidene fluoride)/poly(thiophene) blend nanosheets. RSC Adv. 2018;8:7963–8.
12. Zhang X, Tong J, Zhu H, Wang Z, Zhou L, Wang S, et al. Room temperature magnetoresistance effects in ferroelectric poly(vinylidene fluoride) spin valves. J Mater Chem C. 2017;5:5055–62.
13. Miyashita T, Mizuta Y, Matsuda M. Studies on Langmuir–Blodgett multilayer formation from preformed poly(*N*-alkylacrylamides). Br Polym J. 1990;22:327–31.
14. Zhu H, Matsui J, Yamamoto S, Miyashita T, Mitsuishi M. Solvent-dependent properties of poly(vinylidene fluoride) monolayers at the air–water interface. Soft Matter. 2015;11:1962–72.
15. Nakajima T, Abe R, Takahashi Y, Furukawa T. Intrinsic switching characteristics of ferroelectric ultrathin vinylidene fluoride/trifluoroethylene copolymer films revealed using Au electrode. Jpn J Appl Phys. 2005;44:L1385.
16. Zhu L, Wang Q. Novel ferroelectric polymers for high energy density and low loss dielectrics. Macromolecules. 2012;45:2937–54.
17. Zhou Y, Chan HK, Lam CH, Shin FG. Mechanisms of imprint effect on ferroelectric thin films. J Appl Phys. 2005;98:024111.
18. Nakajima T, Takahashi Y, Okamura S, Furukawa T. Nanosecond switching characteristics of ferroelectric ultrathin vinylidene fluoride/trifluoroethylene copolymer films under extremely high electric field. Jpn J Appl Phys. 2009;48:09KE04.
19. Chu B, Zhou X, Ren K, Neese B, Lin M, Wang Q, et al. A dielectric polymer with high electric energy density and fast discharge speed. Science. 2006;313:334–6.
20. Xie Y, Jiang W, Fu T, Liu J, Zhang Z, Wang S. Achieving high energy density and low loss in PVDF/BST nanodielectrics with enhanced structural homogeneity. ACS Appl Mater Interfaces. 2018;10:29038–47.
21. Budianto Y, Aoki A, Miyashita T. Ultrathin polymer film capacitor composed of poly(*N*-alkylacrylamide) Langmuir–Blodgett films. Macromolecules. 2003;36:8761–5.